Earth and Space Science

Combining In Situ and Satellite Observations to Understand the Vertical Structure of Tropical Anvil Cloud Microphysical Properties During the TC4 Experiment

Qing Yue[1] [ID]**, Jonathan H. Jiang[1]** [ID]**, Andrew Heymsfield[2], Kuo-Nan Liou[3], Yu Gu[3]** [ID]**, and Arushi Sinha[3]**

[1]Jet Propulsion Laboratory, California Institute of Technology, Pasadena, CA, USA, [2]Mesoscale and Microscale Meteorology, National Center for Atmospheric Research, Boulder, CO, USA, [3]Department of Atmospheric and Oceanic Sciences and Joint Institute for Regional Earth System Science and Engineering, University of California, Los Angeles, CA, USA

Abstract Tropical anvil clouds have a profound impact on Earth's weather and climate. Their role in Earth's energy balance and hydrologic cycle is heavily modulated by the vertical structure of the microphysical properties for various hydrometeors in these clouds and their dependence on the ambient environmental conditions. Accurate representations of the variability and covariability of such vertical structures are key to both the satellite remote sensing of cloud and precipitation and numerical modeling of weather and climate, which remain a challenge. This study presents a new method to combine vertically resolved observations from CloudSat radar reflectivity and Cloud-Aerosol Lidar and Infrared Pathfinder Satellite Observation cloud masks with probability distributions of cloud microphysical properties and the ambient atmospheric conditions from detailed in situ measurements on tropical anvils sampled during the National Aeronautics and Space Administration TC4 (Tropical Composition, Cloud and Climate Coupling) mission. We focus on the microphysical properties of the vertical distribution of ice water content, particle size distributions, and effective sizes for different hydrometeors, including ice particles and supercooled liquid droplets. Results from this method are compared with those from in situ data alone and various CloudSat/Cloud-Aerosol Lidar and Infrared Pathfinder Satellite Observation cloud retrievals. The sampling limitation of the field experiment and algorithm limitations in the current retrievals is highlighted, especially for the liquid cloud particles, while a generally good agreement with ice cloud microphysical properties is seen from different methods. While the method presented in this study is applied to tropical anvil clouds observed during TC4, it can be readily employed to study a broad range of ice clouds sampled by various field campaigns.

1. Introduction

The vertically inhomogeneous structures of clouds are important considerations for theoretical cloud modeling, satellite remote sensing, and in situ observations (e.g., Feofilov et al., 2015; Grabowski et al., 2019; Hashino et al., 2013; Korolev et al., 2017; Reinhart et al., 2014; Seo & Biggerstaff, 2006). Often, the inhomogeneous structures of clouds are quantitatively represented by the vertical variability of microphysical properties for different hydrometeor species in the atmosphere, which often vary over certain range and covary with each other. Such variability and covariability are further influenced by the thermodynamic and dynamic environment. Accurate representation of the variability and covariability of the cloud microphysical vertical structures is key to both satellite remote sensing of cloud and precipitation and numerical modeling of weather and climate, which remain a challenge. However, cycling and recycling of energy, water, and chemical species through Earth's atmosphere is critically affected by the variability of cloud properties, especially convective clouds, and its coupling with atmosphere.

Active spaceborne sensors, such as the CloudSat and Cloud-Aerosol Lidar and Infrared Pathfinder Satellite Observation (CALIPSO), provide vertical reflectivity and backscatter profiles with nearly global coverage. Since the launch of CloudSat and CALIPSO, the vertical structures of cloud and precipitation have been extensively studied (Stephens et al., 2018; Winker et al., 2010). Both the radiometric observations and the

retrieval products from these active sensors have been used to investigate the vertical distribution of cloud macrophysical properties such as cloud amount, vertical overlapping structure, and cloud thermodynamic phase and cloud water path (e.g., Bodas-Salcedo, 2014; Bodas-Salcedo et al., 2016; Chepfer et al., 2014; Nair & Rajeev, 2014; Oreopoulos et al., 2017; Stubenrauch et al., 2008) and cloud radiative properties such as optical thickness and radiative forcing (e.g., Haynes et al., 2013; Mace & Wrenn, 2013), which have provided new insights on the microphysical processes of cloud and precipitation (Forbes & Ahlgrimm, 2014; Palerme et al., 2017; Suzuki et al., 2010; Takahashi et al., 2017). However, the radar reflectivity and lidar backscattering profiles alone do not uniquely specify cloud microphysical properties and often rely on apriori assumptions of clouds and cloud-atmosphere relations to perform retrievals from which the cloud property vertical profiles are calculated (e.g., Comstock et al., 2013; Deng et al., 2010). These issues add ambiguity to the interpretation of the vertical variability of cloud microphysical properties and their covariability using the currently available CloudSat/CALIPSO cloud property retrievals.

Field campaigns provide detailed information about the vertical variability of the ice and liquid phase microphysicas using various optical particle probes and their bulk properties together with measurements of the coincident atmospheric conditions. These particle probe measurements, after carefully removing and correcting for measurement artifacts (Baumgardner et al., 2017) have been widely used to understand vertical profiles of ice water content (IWC) and particle shape and size distributions for hydrometeors in various cloud systems by statistically relating the bulk properties of cloud microphysical parameters with environment states, which serves as the basis for cloud parameterizations in numerical models and a priori for satellite retrieval algorithms of both passive (e.g., Elsaesser et al., 2016; Seo & Biggerstaff, 2006; Wang et al., 2019) and active sensors (Deng et al., 2015; Iguchi et al., 2010; Jiang et al., 2019, 2017). However, the vertical profiles obtained from the in situ data may not represent the complete natural variability of microphysical properties due to its sampling statistics and different particle size ranges probes are sensitive to (e.g., Lawson et al., 2010), although measurements in numerous geographical locations have been made (Heymsfield et al., 2017). The issue of sampling statistics is particularly crucial for vertical structures of hydrometeor microphysics. During a typical field campaign, the aircraft sampling is seldom random and complete, partly due to aircraft limitations and the multiple objectives of the field campaign. This brings additional difficulties to characterize the vertical structure of cloud microphysical properties and their relationships with atmospheric conditions from observations.

Therefore, it is important to develop new methodologies that combine the strength of spaceborne active sensors and the detailed in situ observations from field campaigns to examine the variability and covariability of the cloud microphysical properties. These matrices are particularly important for advancing the retrieval of cloud vertical structures. In this study we examine the vertical structures of the cloud microphysical properties for tropical anvil clouds obtained from various data sources and methods including using field campaign measurements alone, from different cloud retrieval products of CloudSat and CALIPSO and from our method that combines the probability distribution functions (pdfs) of cloud microphysical properties with vertical information from active satellite sensors. Tropical anvil clouds and cirrus clouds are chosen to be the focus of this study due to their high frequency of occurrence, and the significant impact of their microphysical properties on cloud radiative forcing, and hence global climate (Hartmann, 2016; Hartmann & Berry, 2017; Hartmann et al., 2018; Stackhouse & Stephens, 1991; Su et al., 2017; Wall et al., 2017; Yue et al., 2019). Moreover, recently developed Tropospheric Water and Cloud ICE (Jiang et al., 2017) instrument and the Earth's NexT-generation ICE (Jiang et al., 2019) SmallSat mission concept present new potentials of retrieving ice and supercooled liquid water particle mass and size distribution vertical profiles in these cloud systems using miniature radiometers and cloud radars. The correlation matrices examined in this study are a crucial component of the retrieval simulation package for these two new systems, which serves as the basis of the a priori in the retrieval.

2. Data and Methodology

The cloud microphysical measurements taken during National Aeronautics and Space Administration's TC4 (Tropical Composition, Cloud and Climate Coupling) mission are used in this study. TC4 is the first major, multiaircraft, comprehensive investigation of tropical anvil clouds. Table 1 lists the flight time of the National Aeronautics and Space Administration DC-8 and WB57 sampling aircraft by cloud type during

Table 1
Cloud Types and Flight Time During TC4 (Lawson et al., 2010)

Cloud types	Time in cloud
Convective turrets	2.35 min
Fresh anvils	48 min
Aged anvils	243 min
In situ cirrus	119 min

TC4, indicating good sample sizes given probe sampling rates on the order of seconds (Lawson et al., 2010). The in situ ice particle size distributions were collected with a two-dimensional stereo (2D-S) probe on the DC-8 and WB-57 aircraft and the precipitation imaging probe (PIP) on the DC-8. 2D-S has a 10-μm pixel resolution at jet speed with 1-s temporal sampling rate and the PIP has a 100-μm pixel resolution with a 5-s sampling rate. Therefore, the 1-s 2D-S data are averaged to 5-s samples to match the PIP. Both data from DC-8 and WB-57 are used in this study to include the ice particles at a colder temperature and higher altitude than measurements made by DC-8 alone. Previous studies such as Lawson et al. (2010) and Baumgardner et al. (2017) have documented the characteristics of cloud types measured during TC4 and measurement quality obtained from the optical probes used in TC4.

The key microphysical properties in our study include the vertical distribution of the particle size distributions, bulk mass for different types of hydrometeors (IWC for ice particles; LWC: liquid water content for liquid particles), bulk effective particle size, and width of the size distribution by fitting gamma size distribution to the particle size distribution. We use equivalent mass spherical diameter for D_e to characterize the particle size. The bulk particle size is the mass weighted mean D_e (D_{me}) and the width of size distribution is measured by the D_e dispersion, D_{e_disp}, where $N(D_e)$ is particle number density as a function of D_e following Evans et al. (2012) and Jiang et al. (2019):

$$D_{me} = \frac{\int N(D_e) D_e^3 D_e dD_e}{\int N(D_e) D_e^3 dD_e} \quad D_{e,disp} = \frac{1}{D_{me}} \left[\frac{\int N(D_e) D_e^3 (D_e - D_{me})^2 dD_e}{\int N(D_e) D_e^3 dD_e} \right]^{1/2} \quad (1)$$

Both 2D-S and PIP probes measure shadowgraphs of the particle from which the particle maximum diameter (D_{max}) and projected area (A) are derived. Conversions between the D_{max} and D_e and between A and D_e follow the power law relationships in Evans et al. (2012) for four nonspherical shapes common in the convective clouds based on the field campaign particle images, including plate aggregates, sphere aggregates, snow aggregates, and solid spheres. Although the shape of ice particles has been shown to be important in the assumptions used in satellite retrieval algorithms (e.g., Mishchenko et al., 1996), which affects uncertainties of the derived moments from the cloud microphysics probe measurements (Baumgardner et al., 2017), and is linked to the physical processes of particle formation and evolution (Lawson et al., 2010), in this study, these aforementioned shapes are assumed and allowed random mixture of particles. Liquid cloud droplets are assumed to be spheres.

The ice particle in situ measurements are quality controlled by removing measurements with $IWC < 10^{-5}$ g/m^3. Supercooled liquid water measurements from the Cloud and Aerosol Spectrometer probe on the DC-8 during TC4 are used by selecting samples within the temperature range of 240 to 273 K (linearly scaled by temperature in this range), $IWC > 10^{-6}$ g/m^3 when measurements from Rosemount Icing Detector (Mazin et al., 2001) indicate presence of supercooled liquid. These thresholds and the measurements from Rosemount Icing Detector are used in the attempt to reduce the ice particle contamination and detect the supercooled liquid water. Temperature is taken from the MMS measurements and humidity is from the diode laser hygrometer and Jet Propulsion Laboratory laser hydrometer that are matched with the microphysical measurements. Vertical variability and covariability of cloud properties are then quantitatively represented using Gaussian distributions and covariance matrices that are derived from the in situ measurements for (1) temperature, RH, ln (IWC), ln (D_{me}), and D_{e_disp} for ice particles, and (2) temperature, RH, ln (IWC), ln (LWC), ln (D_{me_liq}), and $D_{e\_disp\_liq}$ for supercooled liquid water droplets.

To combine the in situ observations with the spaceborne active sensor measurements, first, scattering properties for randomly oriented ice particles and for spherical liquid particles are generated at the 94-GHz CloudSat radar frequency using the discrete diplole approximation for ice particles with the four shapes given in previous discussion and Mie scattering calculation for spherical liquid particles (Evans et al., 2012). Each scattering table includes extinction, single scattering albedo, and Legendre coefficients of the phase function for gamma size distributions as a function of temperature, size (D_{me} and D_{e_disp}), and particle shape. The scattering tables are used to link the microphysical parameters and CloudSat radar reflectivity by creating

a two-dimensional lookup table, which contains the mean vector and covariance matrices for microphysical properties and radar extinction due to particles in the space of radar reflectivity and temperature (e.g., Seo & Liu, 2005). The tables are made by randomly sampling the Gaussian distributions of microphysical properties from in situ observations so that the microphysical properties of hydrometeors are consistent with the radar reflectivity and temperature while constrained by field campaign based statistics. Another advantage of relating field campaign and satellite observations through this approach is that it does not require exact collocation in time and space between in situ and satellite observations since the method uses the pdfs and covariance of the parameters from in situ observations.

Forty-one CloudSat/CALIPSO orbits that intersect the region from 4°N to 12°N and 90°W to 80°W in July and August 2007 are included in this study to be coincident with the TC4 experiments. CloudSat reflectivity within three range gates of the surface elevation is not used to avoid the surface clutter contamination. Above the freezing level, for conditions below the radar sensitivity threshold of −26 dBZ but cloud fraction >50% according to the CALIPSO cloud mask, we used the same method as in Evans et al. (2012) and Jiang et al. (2019) to extend the lookup table to include thin and high cirrus cloud particles. The lookup table is combined with the vertical correlation matrix generated from radar reflectivity profiles to generate independent stochastic hydrometeor parameter profiles for each radar reflectivity profile that have statistics consistent with the in situ microphysics measurements. The coincident temperature and relative humidity profiles for satellite profiles are obtained from CloudSat European Centre for Medium-Range Weather Forecasts (ECMWF)-AUX data sets, which contains ECMWF state variable data interpolated to CloudSat cloud radar bin.

Because during TC4 there is rarely flight penetrating convective cores, below the freezing level (~4.5 km) the precipitation and warm cloud particle distribution is assumed to follow a melting model of ice particles (Bauer et al., 2000; Evans et al., 2012), which may not accurately represent these hydrometeors at these levels. However, since the goal of this study is the ice particles in the tropical anvil clouds and cirrus clouds, impact of this assumption on our results should be minimal.

For comparison purposes, the covariance matrices of various cloud microphysical properties are also derived from different CloudSat/CALIPSO retrieval products, which use different retrieval algorithms and auxiliary measurements such as from MODIS (Moderate Resolution Imaging Spectroradiometer) and ECMWF. Three products are included in this study: (a) CloudSat Radar-Only Cloud Water Content Product (2B-CWC-RO), (b) CloudSat Radar-Visible Optical Depth Cloud Water Content Product (2B-CWC-RVOD), and (c) CloudSat level-2C ice cloud property product (2C-ICE). The 2B-CWC-RO product contains retrievals of cloud liquid and IWC, effective radius of the ice and liquid particles, number concentration, and the size distribution width parameter using radar and auxiliary temperature data (Austin et al., 2009; Wood, 2018). Retrievals are performed separately for the liquid and ice phases assuming liquid only and ice only, respectively, which uses a temperature dependent a priori of the size distribution parameters. The a priori analysis is based on the use of lognormal size distribution fitted from in situ particle size spectra measured during the ARM 2000 Cloud IOP, the AIRS experiment, and CRYSTAL-FACE for ice and those reported in Miles et al. (2000) for liquid. The partition of ice and liquid is purely based on temperature, and the solutions of ice and liquid are scaled linearly with temperature to obtain a smooth transition from all ice at −20 °C to all liquid at 0 °C. Previous studies have shown such composite profiles do not accurately capture the mixed phased cloud structure (Barker et al., 2008). The limited sensitivity of radar reflectivity to small ice particles and thin clouds causes the lower boundary of detection range on roughly 1- to 5-mg/m^3 IWC, while the retrieved LWC is usually nonconvergent in heavy precipitating clouds (Christensen et al., 2013). Validation studies with aircraft measurements reported a relatively good agreement for IWC distribution (Barker et al., 2008) with a conservative bias estimate of 40% (Heymsfield et al., 2008) for the 2B-CWC-RO ice cloud retrievals, while the liquid cloud retrievals suffer a higher uncertainty.

The 2B-CWC-RVOD product produces a similar set of variables with 2B-CWC-RO. The algorithm uses the same a priori assumptions of the particle size distributions and cloud phase determination method with 2B-CWC-RO, however, with additional input auxiliary data on visible optical depth from MODIS (from the CloudSat 2B-TAU product) to more tightly constrain the retrievals (Wood, 2018). When the auxiliary MODIS data are not available such as nighttime or unsuccessful optical depth retrieval, the radar only retrieval is provided. A detailed comparison on the liquid water between the RVOD and MODIS cloud liquid

water shows RVOD underestimates approximately 45% of warm clouds mostly due to the radar ground clutter (Christensen et al., 2013). For the type of clouds focused in this study, the RVOD product suffers from uncertainties and biases similar to the radar only product.

More accurate retrievals on ice cloud microphysical properties are available from the CloudSat/CALIPSO 2C-ICE and radar-lidar (DARDAR) product, which are synergetic ice cloud retrieval derived from the combination of the CloudSat radar reflectivity and the CALIPSO lidar attenuated backscatter (Delanoë & Hogan, 2008, 2010; Deng et al., 2015, 2010). Vertical profiles of extinction coefficient, IWC, and ice particle effective radius are provided by this product. Deng et al. (2013) compared the various CloudSat ice cloud microphysical retrievals with the in situ data collected during the Small Particles in Cirrus field campaign, who found the ice particle effective size from 2B-CWC-RVOD is significantly biased larger than 2C-ICE, DARDAR, and in situ observations by about 40%. Their results indicate that ice cloud properties from 2C-ICE agree with in situ data slightly better than DARDAR, which is contributed by the different treatments of parameterization of radar signals below the detection thresholds and the differences in assumed mass-size and area-size relationships used in the two algorithms. Despite the small differences, a close agreement between 2C-ICE and DARDAR ice cloud retrievals is noticed. Therefore, only 2C-ICE product is included here.

3. Results

Figure 1 shows correlations between variables at different layers and between different variables as a quantitative indicator of the variability and covariability for the vertical structures for ice particles and supercooled liquid water droplets during the TC4 field campaign. Figure 1a shows the results by combining the TC4 microphysical observations on ice and supercooled liquid water with the CloudSat radar reflectivity and CALIPSO cloud mask data as described in the methodology section. Figure 1b shows the correlation calculated directly from in situ observations by compositing TC4 observations into different vertical bins and applying Gaussian fitting to each layer for each variable. Note that the width of the vertical layers is selected so that the histograms of the parameters in each layer follows a near Gaussian distribution. Comparing Figure 1a and Figure 1b, it is clear to see the lack of correlation between temperature and relative humidity at different layers and highly limited vertical range in Figure 1b, which indicates the sampling limitations of the field campaign aircraft measurements. Such sampling limitation also explains the different vertical structures revealed by Figures 1a and 1b on cloud microphysical properties. The results show that by combining in situ and satellite observations we are able to present the entire vertical structures of hydrometeors with a higher vertical resolution from radar, which maintains detailed probability distribution and statistics of parameters from the field campaign observations.

The vertical variability and covariability of the cloud microphysical and atmospheric properties are compared with those derived from retrievals of active satellite sensors: CloudSat and CALISO to investigate how much retrievals from the active sensors are capable to reveal the vertical structure of the cloud particles, especially ice and supercooled liquid water, for which the microphysical properties are directly observed during TC4 using optical probes in Figure 1.

Figure 2 shows the correlation matrices calculated using three different CloudSat/CALIPSO retrieval products: (a) 2B-CWC-RO, (b) 2B-CWC-RVOD, and (c) 2C-ICE. The variables in the figure are temperature and relative humidity from ECMWF-AUX data, retrieved IWC, effective diameter (D_{eff}), and size distribution width for ice particles, LWC, and D_{eff} for liquid water. Since CloudSat retrievals assume spherical particles and the interest of this study is on the covariability structures, no conversions are applied between D_{eff} and D_{me}. Comparing Figure 2 with Figure 1a, consistency between these products and our results on ice clouds is clear while large algorithm differences are also apparent, such as the lack of sensitivity of CloudSat-only retrievals to small particles in thin and high ice clouds, assumptions in liquid only or ice only columns for RO and ROVOD products, as well as ice-only parameters in 2C-ICE. Large differences are seen between 2B-CWC-RO and 2B-CWC-RVOD on the matrices of liquid particles, such as LWC and liquid particle effective diameters, which indicate the ambiguity of the liquid cloud retrievals in these two algorithms. By using the temperature scaling relationship, the vertical extent of liquid portion of the cloud is below 7 km above surface in the CloudSat/CALIPSO products. However, using field campaign data (Figures 1a and 1b), the vertical extent of liquid particles is clearly above 7 km and well into 10-km altitude.
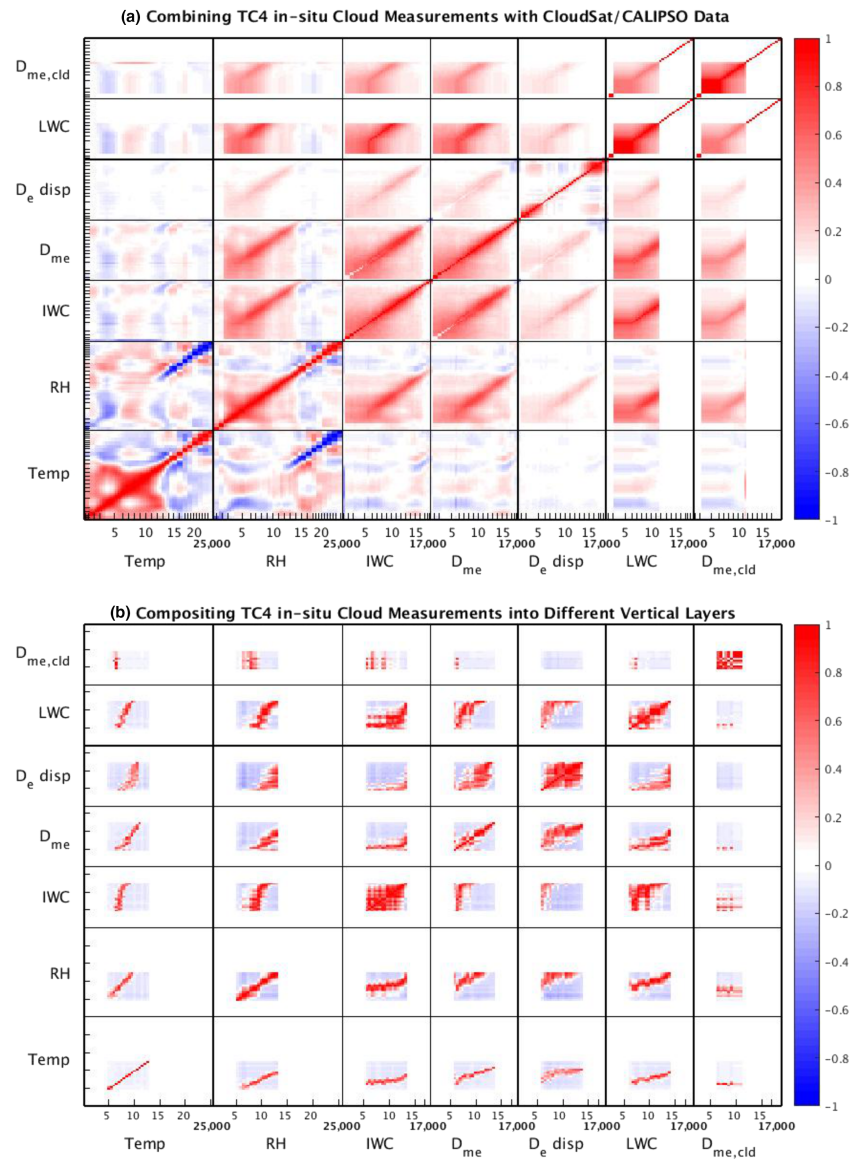
Figure 1. The vertical variability and covariability for ice particles and supercooled liquid water droplets: (a) obtained using the proposed method by combining TC4 cloud microphysics measurements and CloudSat/CALIPSO data (radar reflectivity, lidar cloud mask, collocated ECMWF temperature, and relative humidity); (b) obtained by compositing TC4 cloud microphysics measurements and matched in situ temperature (MMS) and humidity (laser hygrometer) by vertical layers. Color shading shows the correlation coefficients (from −1 to 1). *X* and *y* axes correspond to the vertical levels: 0–25 km for temperature and humidity; 0–17 km for hydrometeors. Note that values below freezing level (~4.5 km) in panel (a) is based on the melting model due to lack of in situ observations in these altitudes during TC4. The variables in the figures are temperature, relative humidity, IWC, D_{me} and D_{e_disp} for ice particles, LWC, and D_{me} for supercooled liquid water above freezing level at 4.5 km. During TC4, the aircraft flight altitude range is ~5 to 12 km, which corresponds with the vertical ranges in panel (b).

The correlation matrices for ice cloud microphysical properties are generally in agreement from different methods, especially for ice clouds below 12 km for both IWC and D_{me}. Above this altitude, a clear temperature and relative humidity dependence of D_{me} is seen from both the combined in situ and satellite method (Figure 1a) and the 2C-ICE (Figure 2c) results, but not in other data products. The dependenc of IWC above 12 km on temperature, on the other hand, is only apparent in the combined method, which agrees with earlier studies based on field campaign data analyses (e.g., Heymsfield et al., 2006; Liou et al., 2008; McFarquhar & Heymsfield, 1997).
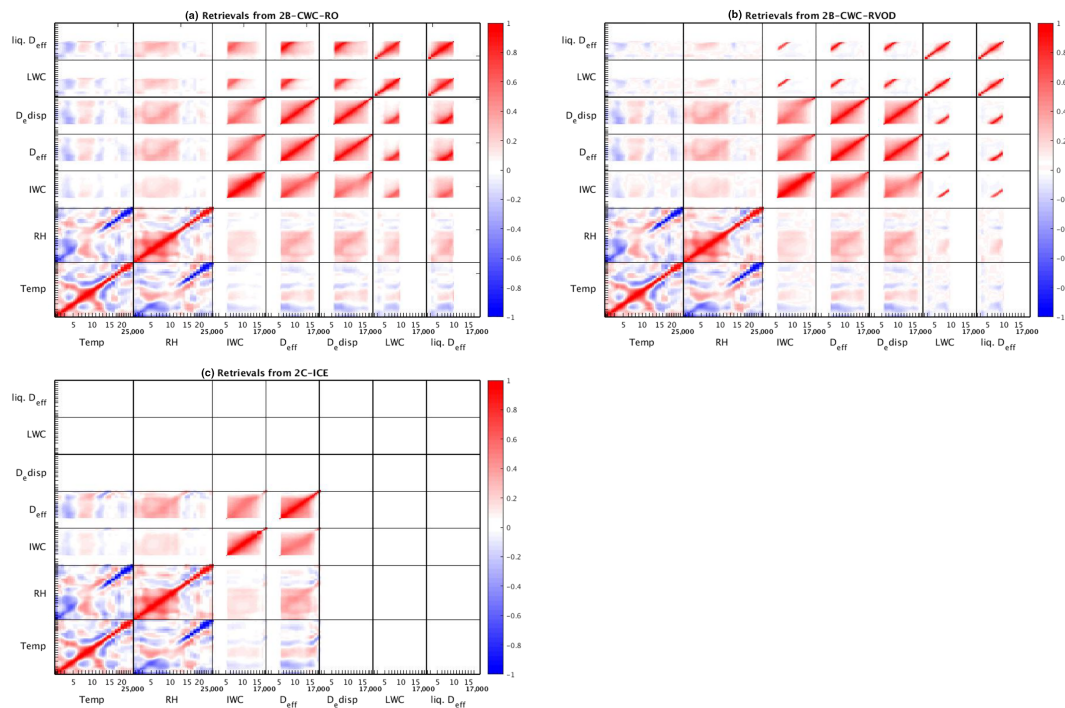
Figure 2. The vertical variability and covariability for ice particles and liquid water droplets obtained from three different CloudSat (CALIPSO) retrieval products over the TC4 region during July and August 2007: (a) 2B-CWC-RO, (b) 2B-CWC-RVOD, and (c) 2C-ICE. Temperature and water profiles are from CloudSat ECMWF-AUX data. Color shading and axis range are the same with Figure 1. The variables in the figures are temperature, relative humidity, IWC, effective diameter (D_{eff}), and size distribution width (D_{e_disp}) for ice particles, LWC, and D_{eff} for liquid water.

4. Summary and Discussions

In spite of increasing attention, representation of cloud properties and microphysical processes in numerical models is nevertheless ambiguous (Boucher et al., 2013; Grabowski et al., 2019; Jiang et al., 2012; Randall et al., 2007; Su et al., 2013). Cloud vertical structures at regional scale are critical in predicting future climate in climate models (Cesana & Chepfer, 2012). Specifically, the vertical variability of cloud ice and liquid phase partitioning in regions where supercooled liquid water droplets and ice particles coexist strongly impacts representation of cloud and precipitation in models (Grabowski et al., 2019; Korolev et al., 2017; McCoy et al., 2016). For satellite remote sensing and in situ observations, the vertical structures of hydrometeors continue to serve as a key component in constructing a priori and developing retrieval algorithms (e.g., Feofilov et al., 2015; Hashino et al., 2013; Jiang et al., 2019; Reinhart et al., 2014; Seo & Biggerstaff, 2006; Wang et al., 2019; Zhang et al., 2010).

The vertical structure of tropical anvil clouds can be quantitatively represented by the vertical variability of microphysical properties for different hydrometeor species in the atmosphere, which often vary over certain range and covary with each other. Such variability and covariability are further influenced by the thermodynamic and dynamic environment. In this study a method is tested to quantify the vertical variability and covariability of cloud microphysical properties of tropical anvil clouds by combining the detailed statistics from in situ optical probe measurements of cloud microphys during the TC4 field experiment with vertical profiles of CloudSat radar reflectivity and CALISPO cloud masks. The simultaneous in situ measurements of hydrometeor microphysics and atmospheric conditions are used to provide the pdf of each parameter and their covariance with each other. These statistics are combined with the vertical correlation matrix provided by active sensor measurements in space to quantify the vertical structure of cloud particles sampled during the TC4 experiments. In addition to the benefit of combining the strength from in situ optical probes and spaceborne active sensors, a strict one-to-one collocation between the satellite and in situ measurements is not necessary in the method; instead, it requires that in situ and spaceborne measurements are from samples with similar cloud types, regions, and season, which is another advantage of our method.

The comparison with the results obtained from three CloudSat/CALIPSO retrieval products on cloud microphysical properties shows the clear algorithm differences on the vertical structures of variability and covariability matrices, which may be related to the assumptions on the correlations among size distribution parameters and between these parameters with temperature, especially for the liquid particles. A detailed examination on how these assumptions may affect the quality of the CloudSat/CALIPSO cloud retrievals is beyond the scope of this study. However, it is encouraging that the current algorithms show consistency on the ice cloud parameters.

The method presented in this study benefits from combining the complemental strengths of in situ cloud microphysical measurements and spaceborne active sensors. Although tropical anvil clouds observed during TC4 are shown in the results, this method can be easily applied to other field campaigns sampling different types of ice clouds. This is not only important to understand the cloud microphysical structures in various cloud systems but also benefits the generalizing and improving of the a priori in the cloud vertical profile retrievals by the Tropospheric Water and Cloud ICE and Earth's NexT-generation ICE retrieval simulation package (Jiang et al., 2019, 2017). The treatment of the liquid hydrometeors including supercooled liquid water and the rain water in the method is limited by the accuracy and availability of the in situ measurements on the microphysical properties of these hydrometeors, which calls for further improvements of in situ observation technologies on these hydrometeor species.

References

Austin, R. T., Heymsfield, A. J., & Stephens, G. L. (2009). Retrieval of ice cloud microphysical parameters using the CloudSat millimeter-wave radar and temperature. *Journal of Geophysical Research*, *114*, D00A23. https://doi.org/10.1029/2008JD010049

Barker, H. W., Korolev, A. V., Hudak, D. R., Strapp, J. W., Strawbridge, K. B., & Wolde, M. (2008). A comparison between CloudSat and aircraft data for a multilayer, mixed phase cloud system during the Canadian CloudSat-CALIPSO Validation Project. *Journal of Geophysical Research: Atmospheres*, *113*, D00A16.

Bauer, P., Khain, A., Pokrovsky, A., Meneghini, R., Kummerow, C., Marzano, F., & Poieres Baptista, J. P. V. (2000). Combined cloud microwave radiative transfer modeling of stratiform rainfall. *Journal of the Atmospheric Sciences*, *57*, 1082–1104.

Baumgardner, D., Abel, S. J., Axisa, D., Cotton, R., Crosier, J., Field, P., et al. (2017). Cloud ice properties: In situ measurement challenges. *Meteorological Monographs*, *58*, 9.1–9.23. https://doi.org/10.1175/AMSMONOGRAPHS-D-16-0011.1

Bodas-Salcedo, A., and Coauthors, 2014: Origins of the solar radiation biases over the Southern Ocean in CFMIP2 models. *Journal of Climate*, *27*, 41–56, https://doi.org/10.1175/JCLI-D-13-00169.1.

Bodas-Salcedo, A., Hill, P. G., Furtado, K., Williams, K. D., Field, P. R., Manners, J. C., et al. (2016). Large contribution of supercooled liquid clouds to the solar radiation budget of the Southern Ocean. *Journal of Climate*, *29*, 4213–4228. https://doi.org/10.1175/JCLI-D-15-0564.1

Boucher, O., Randall, D., Artaxo, P., Bretherton, C., Feingold, G., Forster, P., et al. (2013). Clouds and aerosols. In T. F. Stocker, D. Qin, G. K. Plattner, M. Tignor, S. K. Allen, J. Boschung, A. Nauels, Y. Xia, V. Bex, & P. M. Midgley (Eds.), *Climate change 2013: The physical science basis. Contribution of Working Group I to the Fifth Assessment Report of the Intergovernmental Panel on Climate Change* (Chapter 7, pp. 571–657). Cambridge, UK and New York, NY, USA: Cambridge University Press.

Cesana, G., & Chepfer, H. (2012). How well do climate models simulate cloud vertical structure? A comparison between CALIPSO-GOCCP satellite observations and CMIP5 models. *Geophysical Research Letters*, *39*, L20803. https://doi.org/10.1029/2012GL053153

Chepfer, H., Noel, V., Winker, D., & Chiriaco, M. (2014). Where and when will we observe cloud changes due to climate warming? *Geophysical Research Letters*, *41*, 8387–8395. https://doi.org/10.1002/2014GL061792

Christensen, M. W., Stephens, G. L., & Lebsock, M. D. (2013). Exposing biases in retrieved low cloud properties from CloudSat: A guide for evaluating observations and climate data. *Journal of Geophysical Research – Atmospheres*, *118*, 12,120–12,131. https://doi.org/10.1002/2013JD020224

Comstock, J. M., Protat, A., McFarlane, S. A., Delanoe, J., & Deng, M. (2013). Assessment of uncertainty in cloud radiative effects and heating rates through retrieval algorithm differences: Analysis using 3 years of ARM data at Darwin, Australia. *Journal of Geophysical Research – Atmospheres*, *118*, 4549–4571. https://doi.org/10.1002/jgrd.50404

Delanoë, J., & Hogan, R. J. (2008). A variational scheme for retrieving ice cloud properties from combined radar, lidar, and infrared radiometer. *Journal of Geophysical Research*, *113*, D07204. https://doi.org/10.1029/2007JD009000

Delanoë, J., & Hogan, R. J. (2010). Combined CloudSat-CALIPSO-MODIS retrievals of the properties of ice clouds. *Journal of Geophysical Research*, *115*, D00H29. https://doi.org/10.1029/2009JD012346

Deng, M., Mace, G. G., Wang, Z., & Berry, E. (2015). CloudSat 2C-ICE product update with a new Z_e parameterization in lidar-only region. *Journal of Geophysical Research – Atmospheres*, *120*, 12,198–12,208. https://doi.org/10.1002/2015JD023600

Deng, M., Mace, G. G., Wang, Z., & Lawson, R. P. (2013). Evaluation of several A-Train ice cloud retrieval products with in situ measurements collected during the SPARTICUS campaign. *Journal of applied meteorology and climatology*, *52*, 1014–1030. https://doi.org/10.1175/JAMC-D-12-054.1

Deng, M., Mace, G. G., Wang, Z., & Okamoto, H. (2010). Tropical Composition, Cloud and Climate Coupling experiment validation for cirrus cloud profiling retrieval using CloudSat radar and CALIPSO lidar. *Journal of Geophysical Research*, *115*, D00J15. https://doi.org/10.1029/2009JD013104

Elsaesser, G. S., Genio, A. D., Jiang, J. H., & van Lier-Walqui, M. (2016). An improved convective ice parameterization for the NASA GISS global climate model and impacts on cloud ice simulation. *Journal of Climate*. https://doi.org/10.1175/JCLI-D-16-0346.1

Evans, K. F., Wang, J. R., O'C Starr, D., Heymsfield, G., Li, L., Tian, L., et al. (2012). Ice hydrometeor profile retrieval algorithm for high-frequency microwave radiometers: Application to the CoSSIR instrument during TC4. *Atmospheric Measurement Techniques*, *5*, 2277–2306. https://doi.org/10.5194/amt-5-2277-2012

Feofilov, A. G., Stubenrauch, C. J., and Delanoë, J., 2015: Ice water content vertical profiles of high-level clouds: Classification and impact on radiative fluxes, *Atmospheric Chemistry and Physics*, *15*, 12327–12344, https://doi.org/10.5194/acp-15-12327-2015, 2015.

Forbes, R. M., & Ahlgrimm, M. (2014). On the representation of high-latitude boundary layer mixed-phase cloud in the ECMWF global model. *Monthly Weather Review*, *142*, 3425–3445. https://doi.org/10.1175/MWR-D-13-00325.1

Grabowski, W. W., Morrison, H., Shima, S., Abade, G. C., Dziekan, P., & Pawlowska, H. (2019). Modeling of cloud microphysics: Can we do better? *Bulletin of the American Meteorological Society*, *100*, 655–672. https://doi.org/10.1175/BAMS-D-18-0005.1

Hartmann, D. L. (2016). Tropical anvil clouds and climate sensitivity *Proc. National Academy of Sciences*. https://doi.org/10.1073/pnas.1610455113

Hartmann, D. L., & Berry, S. E. (2017). The balanced radiative effect of tropical anvil clouds. *Journal of Geophysical Research – Atmospheres*. https://doi.org/10.1002/2017JD026460

Hartmann, D. L., Gasparini, B., Berry, S. E., & Blossey, P. N. (2018). The life cycle and net radiative effect of tropical anvil clouds. *Journal of Advances in Modeling Earth Systems*, *10*, 3012–3029. https://doi.org/10.1929/2018MS001484

Hashino, T., Satoh, M., Hagihara, Y., Kubota, T., Matsui, T., Nasuno, T., & Okamoto, H. (2013). Evaluating cloud microphysics from NICAM against CloudSat and CALIPSO. *Journal of Geophysical Research – Atmospheres*, *118*, 7273–7292. https://doi.org/10.1002/jgrd.50564

Haynes, J. M., Vonder Haar, T. H., L'Ecuyer, T., & Henderson, D. (2013). Radiative heating characteristics of Earth's cloudy atmosphere from vertically resolved active sensors. *Geophysical Research Letters*, *40*, 624–630. https://doi.org/10.1002/grl.50145

Heymsfield, A., Krämer, M., Wood, N. B., Gettelman, A., Field, P. R., & Liu, G. (2017). Dependence of the ice water content and snowfall rate on temperature, globally: Comparison of in situ observations, satellite active remote sensing retrievals, and global climate model simulations. *Journal of Applied Meteorology and Climatology*, *56*, 189–215.

Heymsfield, A. J., Schmitt, C., Bansemer, A., van Zadelhoff, G. J., McGill, M. J., Twohy, C., & Baumgardner, D. (2006). Effective radius of ice particle populations derived from aircraft probes. *Journal of Atmospheric and Oceanic Technology*, *23*(3), 361–380. https://doi.org/10.1175/JTECH1857.1

Heymsfield, A. J., et al. (2008). Testing IWC retrieval methods using radar and ancillary measurements with in situ data. *Journal of Applied Meteorology and Climatology*, *47*, 135–163. https://doi.org/10.1175/2007JAMC1606.1

Iguchi T., Seto S., Meneghini R., Yoshida N., Awaka J., and Kubota T. (2010), GPM/DPR level-2 algorithm theoretical basis document, tech. Rep., JAXA–NASA. [Available at http://pps.gsfc.nasa.gov/atbd.html.]

Jiang, J. H., Su, H., Zhai, C., Perun, V. S., Del Genio, A., Nazarenko, L. S., et al. (2012). Evaluation of cloud and water vapor simulations in CMIP5 climate models using NASA A-Train satellite observations. *Journal of Geophysical Research*, *117*, D1410, 24. https://doi.org/10.1029/2011JD017237

Jiang, J. H., Yue, Q., Su, H., Kangaslahti, P., Lebsock, M., Reising, S., et al. (2019). Simulation of remote sensing of clouds and humidity from space using a combined platform of radar and multifrequency microwave radiometers. *Earth and Space Science*, *6*(7), 1234–1243. https://doi.org/10.1029/2019EA000580

Jiang, J. H., Yue, Q., Su, H., Reising, S. C., Kangasalahti, P. P., Deal, W. R., et al. (2017). A simulation of ice cloud particle size, humidity and temperature measurements from the TWICE CubeSat. *Earth and Space Science*. https://doi.org/10.1002/2017EA000296

Korolev, A., McFarquhar, G., Field, P. R., Franklin, C., Lawson, P., Wang, Z., et al. (2017). Mixed-phase clouds: Progress and challenges. *Meteorological Monographs*, *58*, 5.1–5.50. https://doi.org/10.1175/AMSMONOGRAPHS-D-17-0001.1

Lawson, R. P., Jensen, E., Mitchell, D. L., Baker, B., Mo, Q., & Pilson, B. (2010). Microphysical and radiative properties of tropical clouds investigated in TC4 and NAMMA. *Journal of Geophysical Research*, *115*, D00J08. https://doi.org/10.1029/2009JD013017

Liou, K. N., Gu, Y., Yue, Q., & McFarguhar, G. (2008). On the correlation between ice water content and ice crystal size and its application to radiative transfer and general circulation models. *Geophysical Research Letters*, *35*, L13805. https://doi.org/10.1029/2008GL033918

Mace, G. G., & Wrenn, F. (2013). Evaluation of the hydrometeor layers in the east and West Pacific within ISCCP cloud-top pressure–optical depth bins using merged *CloudSat* and *CALIPSO* data. *Journal of Climate*, *26*, 9429–9444. https://doi.org/10.1175/JCLI-D-12-00207.1

Mazin, I. P., Korolev, A. V., Heymsfield, A., Isaac, G. A., & Cober, S. G. (2001). Thermodynamics of icing cylinder for measurements of liquid water content in supercooled clouds. *Journal of Atmospheric and Oceanic Technology*, *18*, 543–558. https://doi.org/10.1175/15200426(2001)018<0543:TOICFM>2.0.CO;2

McCoy, D. T., Tan, I., Hartmann, D. L., Zelinka, M. D., & Storelvmo, T. (2016). On the relationships among cloud cover, mixed- phase partitioning, and planetary albedo in GCMs. *Journal of Advances in Modeling Earth Systems*, *8*, 650–668. https://doi.org/10.1002/2015MS000589

McFarquhar, G., & Heymsfield, A. (1997). Parameterization of tropical cirrus ice crystal size distributions and implications for radiative transfer: Results from CEPEX. *Journal of the Atmospheric Sciences*, *54*, 2187–2200.

Miles, N. L., Verlinde, J., & Clothiaux, E. E. (2000). Cloud droplet size distributions in low-level strati-form clouds. *Journal of the Atmospheric Sciences*, *57*, 295–311.

Mishchenko, M. I., Rossow, W. B., Macke, A., & Lacis, A. A. (1996). Sensitivity of cirrus cloud albedo, bidirectional reflectance and optical thickness retrieval accuracy to ice particle shape. *Journal of Geophysical Research*, *101*, 16,973–16,985. https://doi.org/10.1029/96JD01155

Nair, A. K., & Rajeev, K. (2014). Multiyear CloudSat and CALIPSO observations of the dependence of cloud vertical distribution on sea surface temperature and tropospheric Dynamics. *Journal of Climate*, *27*, 672–683. https://doi.org/10.1175/JCLI-D-13-00062.1

Oreopoulos, L., Cho, N., & Lee, D. (2017). New insights about cloud vertical structure from CloudSat and CALIPSO observations. *Journal of Geophysical Research – Atmospheres*, *122*(17), 9280–9300. https://doi.org/10.1002/2017JD026629

Palerme, C., Genton, C., Chaud, C., Kay, J. E., Wood, N. B., & L'Ecuyer, T. (2017). Evaluation of current and projected Antarctic precipitation in CMIP5 models. *Climate Dynamics*, *48*(1-2), 225–239. https://doi.org/10.1007/s00382-016-3071-1

Randall, D. A., Wood, R. A., Bony, S., Colman, R., Fichefet, T., Fyfe, J., et al. (2007). Climate models and their evaluation. In S. Solomon D. Qin, M. Manning, Z. Chen, M. Marquis, K. B. Averyt, M. Tignor, & H. L. Miller (Eds.), *Climate Change 2007: The physical sciences basis contribution of working group I to the fourth assessment report of the inter governmental panel on climate change* (chap 8 pp. 589–662). Cambridge University Press, U. K.

Reinhart, B., Fuelberg, H., Blakeslee, R., Mach, D., Heymsfield, A., Bansemer, A., et al. (2014). Understanding the relationships between lightning, cloud microphysics, and airborne radar-derived storm structure during Hurricane Karl (2010). *Monthly Weather Review*, *142*, 590–605. https://doi.org/10.1175/MWR-D-13-00008.1

Seo, E-K., and G. Liu, 2005: Retrievals of cloud ice water path by combining ground cloud radar and satellite high-frequency microwave measurements near the ARM SGP site. *Journal of Geophysical Research*, *110*.D14203, doi:https://doi.org/10.1029/2004JD005727

Seo, E.-K., & Biggerstaff, M. I. (2006). Impact of cloud model microphysics on passive microwave retrievals of cloud properties. Part II: Uncertainty in rain, hydrometeor structure and latent heating retrievals. *Journal of Applied Meteorology and Climatology*, *45*, 955–972.

Stackhouse, P. W., & Stephens, G. L. (1991). A theoretical and observational study of the radiative properties of cirrus: Results from FIRE 1986. *Journal of the Atmospheric Sciences*, *48*, 2044–2059.

Stephens, G., Winker, D., Pelon, J., Trepte, C., Vane, D., Yuhas, C., et al. (2018). CloudSat and CALIPSO within the A-Train: Ten years of actively observing the Earth system. *Bulletin of the American Meteorological Society*, *99*, 569–581. https://doi.org/10.1175/BAMS-D-16-0324.1

Stubenrauch, C. J., Cros, S., Lamquin, N., Armante, R., Chédin, A., Crevoisier, C., & Scott, N. A. (2008). Cloud properties from Atmospheric Infrared Sounder and evaluation with Cloud-Aerosol Lidar and Infrared Pathfinder Satellite Observations. *Journal of Geophysical Research*, *113*, D00A10. https://doi.org/10.1029/2008JD009928

Su, H., Jiang, J. H., Zhai, C., Perun, V. S., Shen, J. T., Del Genio, A., et al. (2013). Diagnosis of regime-dependent cloud simulation errors in CMIP5 models using "A-Train" satellite observations and reanalysis data. *Journal of Geophysical Research: Atmospheres*, *118*, 2762–2780.

Su, H., Zhang, J. H., Neelin, J. D., Shen, T. J., Zhai, C., Yue, Q., et al. (2017). Tightening of Hadley ascent and tropical high cloud region key to precipitation change in a warmer climate. *Nature Communications*, *8*(1), 1–9. https://doi.org/10.1038/ncomms15771

Suzuki, K., Nakajima, T. Y., & Stephens, G. L. (2010). Particle growth and drop collection efficiency of warm clouds as inferred from joint *CloudSat* and MODIS observations. *Journal of the Atmospheric Sciences*, *67*, 3019–3032. https://doi.org/10.1175/2010JAS3463.1

Takahashi, H., Suzuki, K., & Stephens, G. L. (2017). Land–ocean differences in the warm rain formation process in satellite observations, ground-based observations, and model simulations. *Quarterly Journal of the Royal Meteorological Society*, *143*, 1804–1815. https://doi.org/10.1002/qj.3042

Wall, C. J., Hartmann, D. L., & Ma, P.-L. (2017). Instantaneous linkages between clouds and large-scale meteorology over the Southern Ocean in observations and a climate model. *Journal of Climate*, *30*, 9455–9474.

Wang, C., Platnick, S., Fauchez, T., Meyer, K., Zhang, Z., Iwabuchi, H., & Kahn, B. H. (2019). An assessment of the impacts of cloud vertical heterogeneity on global ice cloud data records from passive satellite retrievals. *Journal of Geophysical Research: Atmospheres*, *124*, 1578–1595. https://doi.org/10.1029/2018JD029681

Winker, D. M., Pelon, J., Coakley, J. A., Ackerman, S. A., Charlson, R. J., Colarco, P. R., et al. (2010). The CALIPSO mission. *Bulletin of the American Meteorological Society*, *91*, 1211–1230. https://doi.org/10.1175/2010BAMS3009.1

Wood, N. 2018, Level 2B Radar-Visible Optical Depth Cloud Water Content (2B-CWC-RVOD) process description document, Available from

Yue, Q. (2020): Generated datasets for Yue et al., (2020, Earth and space science): "Combining in-situ and satellite observations to understand the vertical structure of tropical anvil cloud microphysical properties during the TC4 experiment" [data set]. Earth and Space Science. Zenodo. http://doi.org/10.5281/zenodo.3700059

Yue, Q., Kahn, B. H., Fetzer, E. J., Wong, S., Huang, X., & Schreier, M. (2019). Temporal and spatial characteristics of short-term cloud feedback on global and local interannual climate fluctuations from A-Train observations. *Journal of Climate*, *32*, 1875–1893. https://doi.org/10.1175/JCLI-D-18-0335.1

Zhang, D., Wang, Z., & Liu, D. (2010). A global view of midlevel liquid-layer topped stratiform cloud distribution and phase partition from CALIPSO and CloudSat measurements. *Journal of Geophysical Research*, *115*, D00H13. https://doi.org/10.1029/2009JD012143